ARTICLE

ACS chemical biology

(−)-CHANA, a Fluorogenic Probe for Detecting Amyloid Binding Alcohol Dehydrogenase HSD10 Activity in Living Cells

Kirsty E. A. Muirhead[†,¶], Mary Froemming[‡,¶], Xiaoguang Li[‡,¶], Kamil Musilek[§], Stuart J. Conway[∥], Dalibor Sames[‡,⊥], and Frank J. Gunn-Moore[†,⊥,*]

[†]School of Biology, Medical and Biological Sciences Building, North Haugh, University of St. Andrews, St. Andrews KY16 9TF, United Kingdom, [‡]Department of Chemistry, Columbia University, New York, New York 10027, [§]Department of Toxicology, Faculty of Military Health Sciences, Trebesska 1575, 500 01 Hradec Kralove, Czech Republic, and [∥]Department of Chemistry, Chemistry Research Laboratory, University of Oxford, Mansfield Road, Oxford OX1 3TA, United Kingdom, [⊥]These authors contributed equally to this work., [¶]These authors contributed equally to this work.

ABSTRACT The association of 17β-hydroxysteroid dehydrogenase 10 (HSD10) with β-amyloid in the brain is known to contribute to the progression of Alzheimer's disease. Further, it has been shown that the interaction between the purified HSD10 and β-amyloid inhibits its enzymatic activity. However, to date no system has been developed to enable the study of HSD10 activity in intact living cells. To address this significant shortcoming, we have developed a novel fluorogenic probe, (−)-cyclohexenyl amino naphthalene alcohol [(−)-CHANA], to observe and measure the activity of HSD10 in living cells. The oxidation of (−)-CHANA by HSD10 results in the production and accumulation of a fluorescent product, which can be measured using real-time fluorescence microscopy. This compound permits the measurement of mitochondrial HSD10 activity and its inhibition by both a small molecule HSD10 inhibitor and by β-amyloid, in living cells. Herein, we define the parameters under which this probe can be used. This compound is likely to prove useful in future investigations aimed at developing therapeutic compounds targeting the HSD10-β-amyloid association.

17β-Hydroxysteroid dehydrogenase 10 (HSD10) is an enzyme implicated in the mitochondrial dysfunction associated with Alzheimer's disease (AD) (*1*) (reviewed in ref 10). HSD10 is referred to in the literature by a number of names, including amyloid-binding alcohol dehydrogenase (ABAD) (*1*–*3*), endoplasmic reticulum associated amyloid-binding protein (ERAB) (*4*–*7*), human brain short chain L-3-hydroxyacyl-CoA dehydrogenase (SCHAD) (*8, 9*), and human type II hydroxyacyl-CoA dehydrogenase (HADH II) (*1, 6*). HSD10 shares a number of features with a broad range of short-chain dehydrogenase reductase enzymes, including its conserved catalytic triad of Ser^{155}, Tyr^{168}, and Lys^{172}, and acts on a variety of substrates; its known roles include the third step of the β-oxidation of fatty acids (*2, 11*), isoleucine catabolism (*12*), and steroid metabolism (*5, 13*) (see ref 10 for discussion of the catalytic function of HSD10). It is therefore thought that this enzyme is important in producing energy in glucose-deficient environments and maintaining metabolic homeostasis. In the presence of the peptide β-amyloid (Aβ), which is elevated in the brains of those affected by AD, an HSD10-Aβ complex is formed. This complex leads to increased intracellular production of reactive oxygen species, decreased mitochondrial function, and ultimately cell death (*1, 3, 7, 14*). It is known that Aβ inhibits the activity of purified ABAD protein (*6, 7*); *in vitro*, it has been shown that Aβ distorts HSD10's active site and cofactor binding site, resulting in disruption of the enzyme's normal function (*3, 4, 15*). It has also been demonstrated that interven-

***Corresponding author,**
fjg1@st-and.ac.uk.

Received for review July 1, 2010
and accepted September 13, 2010.
Published online September 13, 2010
10.1021/cb100199m

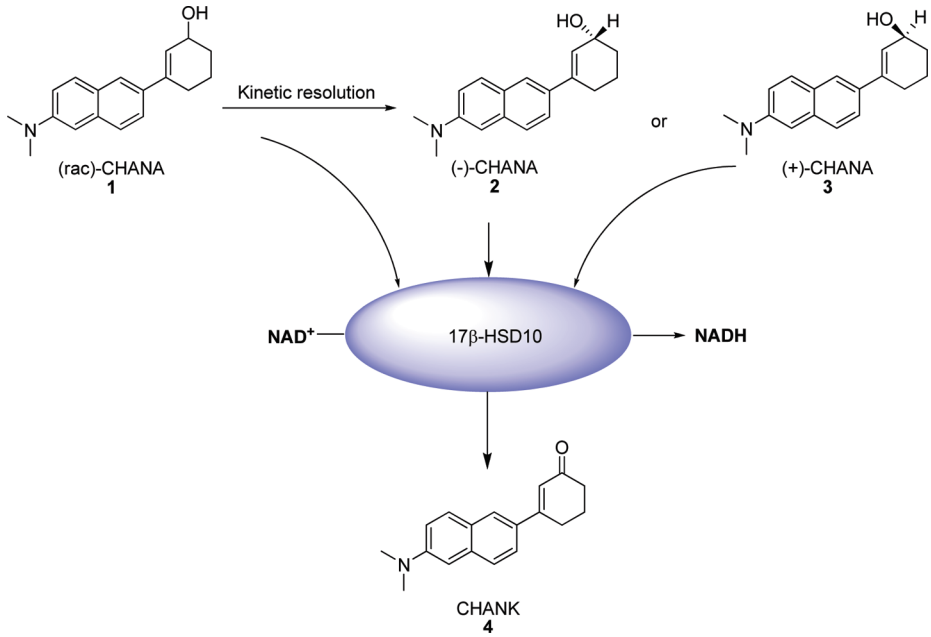

Figure 1. Examining the enantiomers of CHANA, an optical reporter substrate for HSD10. Using NAD$^+$ as a cofactor, HSD10 has been previously shown to catalyze the oxidation of *rac*-CHANA (1) to the ketone, CHANK (4). Kinetic resolution shows HSD10 to be highly selective toward (−)-CHANA (2).

tion of this interaction can have therapeutic benefits in a mouse model of AD (*3, 16, 17*).

To study this enzyme in intact living cells, a fluorogenic probe, CHANA (cyclohexenyl amino naphthalene alcohol), had been developed previously (*18*). CHANA was designed as a reporter substrate for HSD10 to provide fluorescence output for the enzymatic oxidation carried out by this enzyme. In a hydrophobic environment (chloroform solution or cell membranes), CHANA exhibits very low fluorescence, whereas the corresponding ketone product, CHANK (cyclohexenyl amino naphthalene ketone), is highly fluorescent (green-yellow fluorescence, Figure 1). This property allows the enzyme activity in living cells to be monitored in real time using fluorescence microscopy, by measuring the intensity of accumulated CHANK. However, this original substrate was produced in a racemic form and showed significant background oxidation in null-transfected HEK293T cells (*18*). We speculated that one enantiomer of CHANA would likely be a more selective substrate for HSD10 than the other, leading to a reduction in background oxidation and fluorescence. Herein, we report the single enantiomer (−)-CHANA, an improved fluorogenic probe for detecting HSD10 activity, and investigate the potential applications and limitations of its use in measuring HSD10 activity in living systems.

RESULTS AND DISCUSSION

Kinetic Resolution of Racemic (±)-CHANA. To improve CHANA's kinetic parameters and selectivity of metabolism in living cells, we proceeded to prepare both enantiomers of this probe. Although many asymmetric synthetic methods failed, we were able to obtain the separate enantiomers from the racemic CHANA *via* kinetic resolution, using Noyori's ruthenium-catalyzed transfer hydrogenation/oxidation protocol (Figure 2) (*19*). This method relies on differential rates of oxidation of the individual enantiomers by a chiral catalyst, which converts one alcohol enantiomer to the corresponding ketone faster than the other and in favorable cases results in preparation of one enantiomer at a high optical purity. Using the (*S*,*S*)-*N*-*p*-tosyl-1,2-diphenyl-ethylenediamine ligand, the (+)-CHANA enantiomer is oxidized faster, leaving (−)-CHANA in high enantiomeric excess (>96% ee) and 21% yield. It is noteworthy that the recovered CHANK can readily be reduced back to racemic CHANA under Luche conditions (*20*), and the kinetic resolution process can be repeated. The opposite enantiomer (+)-CHANA was also prepared in high enantiomeric excess (>98% ee) by the same kinetic procedure using the enantiomeric (*R*,*R*)-*N*-*p*-tosyl-1, 2-diphenyl-ethylenediamine ligand. The absolute configuration of (−)-CHANA is predicted to be (*R*) according to literature precedent detailing preparation of similar alcohols (*19*).

Enzyme Kinetics. Kinetic parameters for racemic and (+)- and (−)-CHANA were obtained with recombinant purified human HSD10 protein (Table 1). It can be seen that HSD10 has ~10-fold greater activity on (−)-CHANA than on the (+)-enantiomer, along with a much greater catalytic turnover (k_{cat}) and catalytic efficiency (k_{cat}/K_m). These data indicate that (−)-CHANA is a better substrate for HSD10-catalyzed oxidation.

Cellular Activity and Distribution. Previous work has shown that the racemic mixture of CHANA is a substrate

TABLE 1. Kinetic parameters of CHANA probes with HSD10

Substrate	K_m (μM)	SA (μmol min^{-1} g^{-1})	k_{cat} (min^{-1})	k_{cat}/K_m (μM^{-1} min^{-1})
rac-CHANA	12 ± 2	6.0 ± 0.5	200 ± 20	18 ± 3
(+)-CHANA	8 ± 2	0.69 ± 0.1	22 ± 3	2.5 ± 0.7
(−)-CHANA	5 ± 1	6.6 ± 0.9	170 ± 20	48 ± 5

for HSD10 when the enzyme is overexpressed in living HEK293T cells (*18*). With the individual enantiomers (+)-CHANA and (−)-CHANA in hand, we demonstrate that (−)-CHANA is selectively dehydrogenated by HSD10 in living HEK293T cells (Figure 3). (+)-CHANA was shown to be metabolized at similar rates in null-transfected and HSD10-transfected cells, indicating that the presence of additional HSD10 does not lead to increased metabolism of this substrate (Figure 3, panels a and b). Meanwhile, (−)-CHANA was found to exhibit minimal activity in null-transfected cells and much greater levels of metabolism in cells overexpressing HSD10 (Figure 3, panels c and d). Additionally, no oxidation of CHANA was observed in the absence of cells (data not shown). These results, obtained using standard fluorescent microscopy, therefore indicate that HSD10 is highly selective for the (−)-enantiomer.

Studying this system using the more sensitive technique of confocal fluorescence microscopy allowed more detailed observations of the intracellular behavior of the probe to be made. Whereas the null-transfected cells in Figure 3 showed no fluorescence upon treatment with (−)-CHANA, HEK293 cells studied using confocal microscopy exhibited some fluorescence, albeit far less than cells transfected with mitochondrial-targeted HSD10 (MTS-HSD10) (Figure 4, panels a and b). The difference in fluorescence levels correlates to the relative expression levels of HSD10 in null- and MTS-HSD10-transfected cell, as determined by Western blotting (Figure 4, panel c). The use of confocal microscopy therefore potentially allows the activity of endogenous HSD10 to be measured.

During examination of endogenous activity in untransfected HEK293 and SK-N-SH cell lines and primary

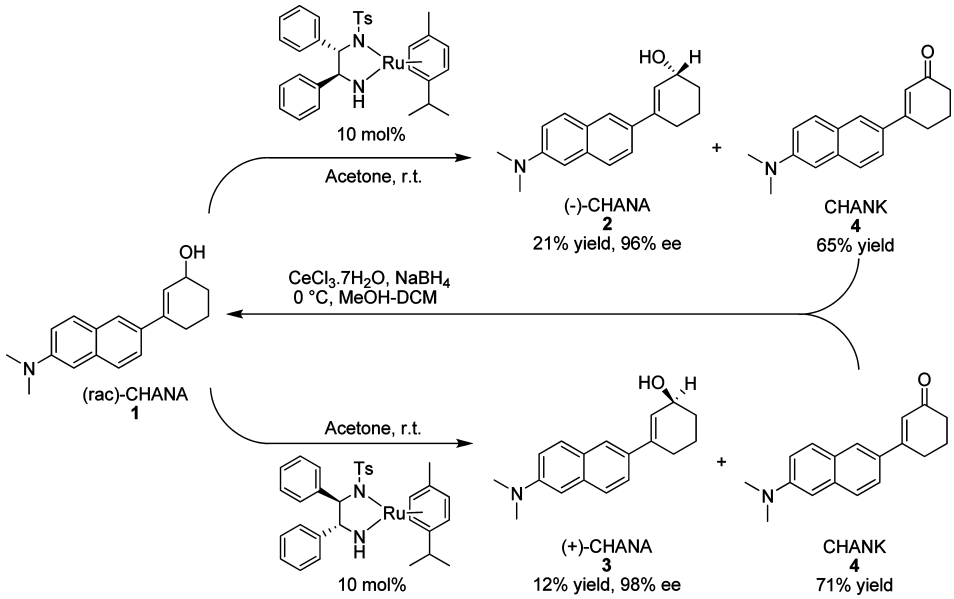

Figure 2. Synthesis of (−)-CHANA and (+)-CHANA enantiomers *via* kinetic resolution of racemic mixture using ruthenium-catalyzed transfer hydrogenation.

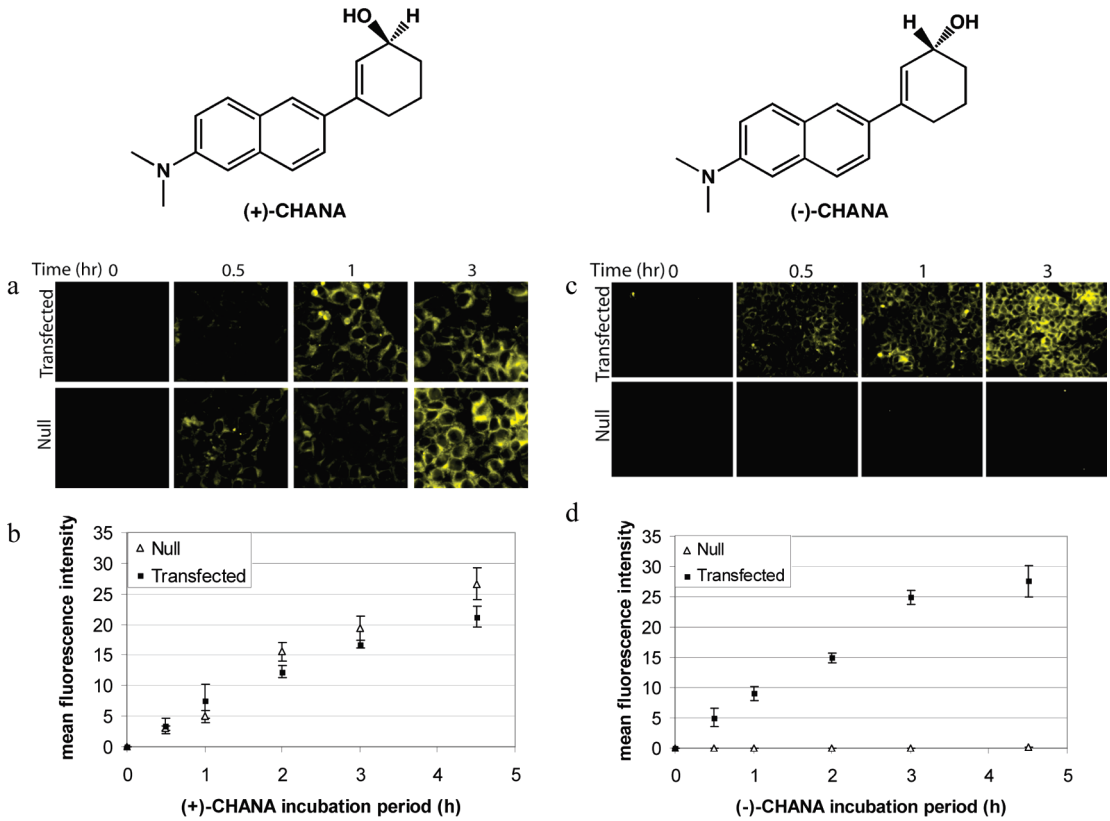

Figure 3. Metabolism of (+)- and (−)-CHANA in HSD10-transfected HEK293T cells. a) Conversion of (+)-CHANA in HSD10 and null transfected cells imaged by fluorescence microscopy and (b) quantified by ImageJ. c) Conversion of (−)-CHANA in HSD10 and null transfected cells imaged by fluorescence microscopy and (d) quantified by ImageJ.

mouse cortical neurons, it became apparent that CHANK staining was not uniform throughout the cell and that distinct areas of staining were visible, corresponding to intracellular structures (see Supplementary Figure S1). Although HSD10 has been located to several cellular environments, including mitochondria, ER, and the cell membrane (*1, 5, 6, 21*), it is mitochondrial HSD10 in particular that has been implicated in the progression of Alzheimer's disease (*1*) (reviewed in ref 10). It was noted with interest that costaining with MitoTracker Deep Red, a mitochondrial dye, revealed co-localization of a proportion of the CHANK fluorescence with the mitochondrial marker, indicating its accumulation within the mitochondria (Figure 5, panel a). As had been expected due to the photochemical properties and hydrophobic nature of the probe, the mitochondrial accumulation is mostly on the outermost surface of the organelle, corresponding to the mitochondrial membrane region, as highlighted by the graphical representation of the cross section of a single mitochondrion (Figure 5, panels b and c).

In addition to mitochondrial staining, non-mitochondrial CHANK accumulation is also apparent. This may result from non-mitochondrial HSD10 activity (see above) or from the redistribution of CHANK into other lipophilic structures within the cell. HSD10 knock-down experiments did not lead to a decrease in fluorescence observed, although complete knock-down was not achieved and the activity resulting from up-regulation of compensatory pathways involving alternative dehydrogenases cannot be ruled out (see Supporting Information).

Our results show that (−)-CHANA can act as a substrate for HSD10 and that the imaging of HSD10 activity in intact cells can be conducted when HSD10 is overexpressed.

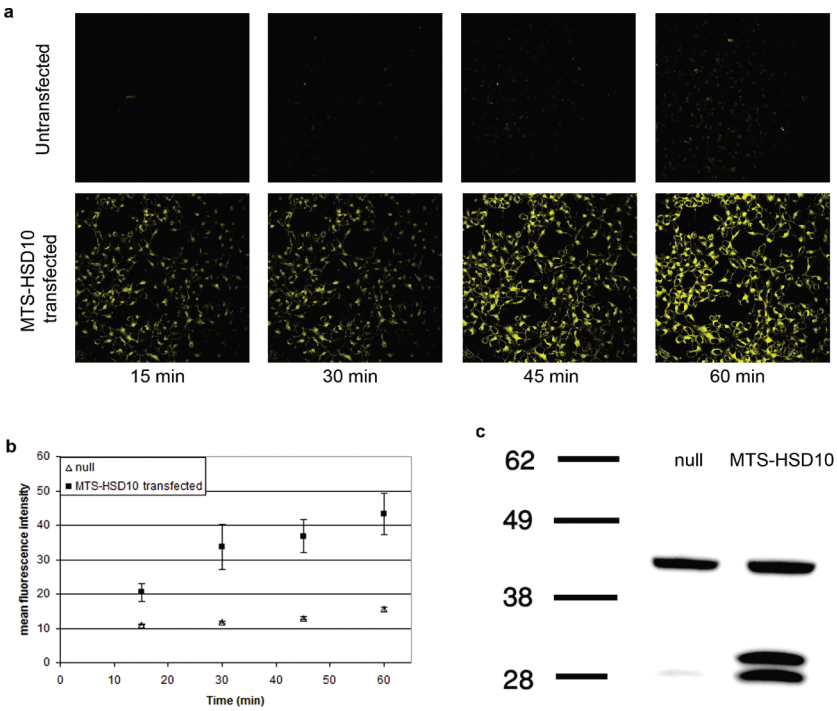

Figure 4. Confocal microscopy studies of (−)-CHANA metabolism in living HEK293T cells. a) HEK293T cells incubated with 2 μM (−)-CHANA: untransfected cells (top) and MTS-HSD10 (mitochondrial-targeted HSD10)-transfected cells (bottom). b) Quantification was performed using ImageJ. Errors are given as SEM. c) Western blot showing null- (Lane 1) or MTS-HSD10-transfected (Lane 2) HEK293 cells. Blotting with anti-HSD10 revealed HSD10 (27 kDa) and MTS-HSD10 (30 kDa). Anti-β-actin (upper band, 42 kDa) was used as a loading control.

Further evidence for the selectivity of HSD10 for (−)-CHANA is shown by the effect of the known HSD10 inhibitor, AG18051 (Figure 6, panel a), on the metabolism of (−)-CHANA. AG18051 is an irreversible inhibitor for HSD10; it occupies the substrate binding pocket and covalently binds to NAD^+ (*4*). By applying AG18051 to our assays, we measured the inhibition of HSD10 utilizing (−)-CHANA, in both null and HSD10-transfected cells (Figure 6, panel b). Monitoring the metabolism of (−)-CHANA in cells, we determined that AG18051 has an IC_{50} value of 140 ± 10 nM, which is similar to the *in vitro* reported value of 92 nM (*4*) (Figure 6, panel c). These data not only demonstrate the selective nature of HSD10 action on (−)-CHANA but also suggest that (−)-CHANA is a useful fluorogenic probe for the identification of new HSD10 inhibitors.

Inhibition of HSD10 by β-Amyloid. HSD10 has a known nanomolar binding site for β-amyloid (Aβ), as demonstrated by techniques including surface plasmon resonance (*3, 15*), immunoprecipitation (*1, 3, 5*), and crystallography (*3*). The binding of Aβ has been shown to inhibit the enzyme by altering the shape of the cofactor binding site (*3, 6, 15*). To date, there has been no measurement of intracellular HSD10 activity in living cells in the presence of Aβ. Therefore, HEK293 cells were transfected with the plasmid encoding MTS-HSD10, and after 24 h, the cells were treated with 22 μM Aβ42 for a further 24 h before incubating with (−)-CHANA for 15−60 min. The fluorescence observed in Aβ-treated cells was significantly (~20%) lower than that of untreated controls ($p = 0.004$ after 60 min; Figure 7), indicating that some inhibition of (−)-CHANA metabolism and hence inhibition of HSD10 activity within the cell was occurring. It appears that there is a window of opportunity for use of Aβ in such an assay: use of higher Aβ concentration (50 μM) results in cell death, whereas with lower concentrations (<10 μM) no inhibition was seen (data not shown).

Conclusions. We report syntheses for both enantiomers of the fluorogenic probe CHANA. It is demonstrated that (−)-CHANA is a selective substrate for 17β-hydroxysteroid dehydrogenase 10 (HSD10), which is an enzyme that enhances the cell toxicity of β-amyloid peptide in Alzheimer's disease. We have identified the parameters under which this novel substrate can be utilized; namely, (−)-CHANA can be used in both *in vitro* enzyme assays or for fluorescence microscopy studies in living cells transfected with HSD10. In addition, using this novel chemical probe, we have shown, for the first time in living cells, that HSD10 activity is reduced by the

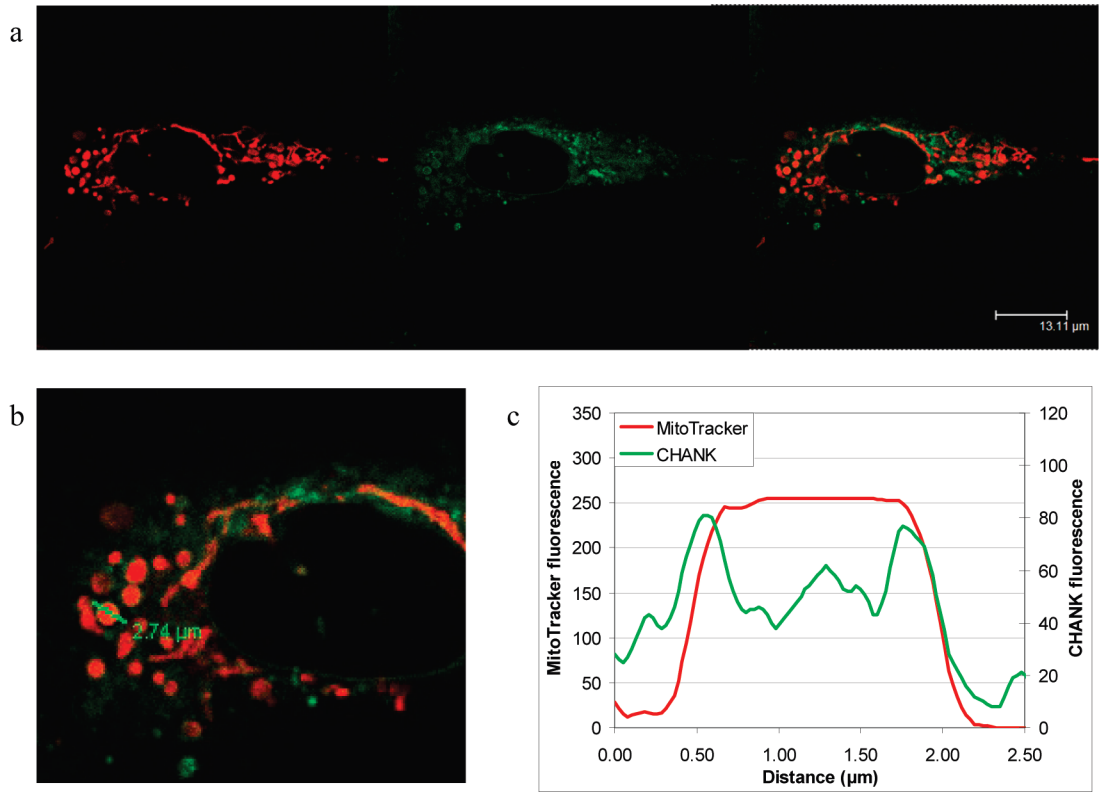

Figure 5. Co-localization of MitoTracker Deep Red (red) and (−)-CHANA metabolism product, CHANK (green), in SK-N-SH cells. a) Cells were stained with MitoTracker Deep Red and then (−)-CHANA before imaging: MitoTracker (red, left), (−)-CHANA (green, center), and merged image (right). b) Close-up of MitoTracker and CHANK fluorescence staining, showing co-localization (yellow/orange) in the mitochondrial membrane. c) Fluorescence intensity of MitoTracker and CHANK along the transect line shown in panel b.

addition of β-amyloid (Aβ). This result is significant as the binding of Aβ to HSD10 has been shown to be a potential site for therapeutic intervention in Alzheimer's disease (*3, 16, 17*). Therefore under these conditions (−)-CHANA is potentially useful for the analysis of new therapeutic compounds to treat Alzheimer's disease.

METHODS

Synthesis of (−)-CHANA and (+)-CHANA Probes. Nuclear magnetic resonance spectra were recorded on Bruker 300 or 400 Fourier transform NMR spectrometers. Chemical shifts are reported as δ values in ppm referenced to $CDCl_3$ (^{1}H NMR = 7.26 and ^{13}C NMR = 77.0). Multiplicity is indicated as follows: s (singlet); d (doublet); t (triplet); q (quartet); dd (doublet of doublets); m (multiplet); bs (broad singlet). Infrared spectra (IR) were obtained as thin films, on a Perkin-Elmer Paragon 1000 FTIR spectrometer and are reported in wavenumbers (cm^{-1}). High-resolution mass spectra (HRMS) were acquired from Columbia University Mass Spectral Core facility on a JMS HX110 spectrometer. Optical rotations were measured on a JASCO DIP-1000 spectrometer.

(−)-CHANA: (−)-3-(6-Dimethylamino-2-naphthyl)-2-cyclohexenol. An 8 mL glass vial was charged with di-μ-chlorobis[(*p*-cymene)chlororuthenium(II)], (30.6 mg, 0.050 mmol) and (*S*,*S*)-*N*-*p*-tosyl-1,2-diphenylethylenediamine (36.6 mg, 0.10 mmol). After purging with argon three times, isopropanol (1.0 mL) was added. The mixture was heated at 80 °C for 0.5 h and then cooled to RT under careful argon protection. NaOH (0.4 mmol, 1.0 mL of a 0.4 M NaOH solution in isopropanol) was introduced, and the mixture was stirred for 5 min at RT. The resulting mixture was then transferred to a Schlenck tube, which was previously charged with the racemic CHANA (267.2 mg, 1.0 mmol) in dry acetone (10 mL) under argon. The mixture was then stirred at RT (typically 5−8 h). An aliquot was removed from the reaction, and a pure sample for HPLC analysis was obtained using preparative TLC. When the reaction reached >95% ee, the volatiles were removed quickly, and further purification was performed by column chromatography (ethyl acetate/dichloromethane, from 1:12 to 1:8) to give alcohol probe (−)-CHANA (55 mg; 21%) as a yellow powder, together with the recovered ketone CHANK (174 mg; 65% yield). ^{1}H NMR (400 MHz, $CDCl_3$): δ 7.73−7.65 (m, 2H), 7.60 (d, J = 8.4 Hz, 1H), 7.51 (dd, J_1 = 8.8

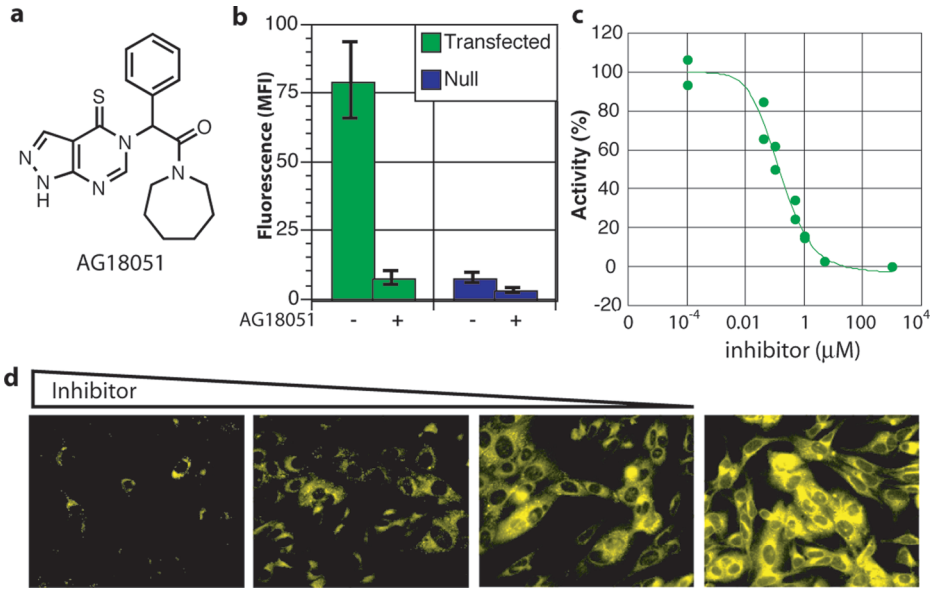

Figure 6. Inhibition of HSD10 by AG18051 in SK-N-SH cells. a) Structure of AG1851. b) Inhibition of the metabolism of (−)-CHANA by AG18051 (1 μM) in HSD10-transfected and null-transfected cells. Bar represents average MFI at 24 h. c) IC_{50} curve of AG18051, as measured by monitoring the oxidation of (−)-CHANA (15 μM) in HSD10 transfected SK-N-SH cells, IC_{50} = 140 ± 10 nM. d) Images of the metabolism of (−)-CHANA in HSD10 transfected cells incubated with AG18051 (5, 1, 0.5, 0 μM), an HSD10 inhibitor.

Hz, J_2 = 2.0 Hz, 1H), 7.15 (dd, J_1 = 8.8 Hz, J_2 = 2.4 Hz, 1H), 6.89 (d, J = 2.0 Hz, 1H), 6.24 (pseudo t, J = 2.0 Hz, 1H), 4.44 (m, 1H), 3.05 (s, 6H), 2.65−2.42 (m, 2H), 2.05−1.88 (m, 2H), 1.85−1.65 (m, 2H), 1.60−1.45 (m, 1H). ^{13}C NMR (75 MHz, $CDCl_3$): δ 148.69, 140.02, 134.56, 134.40, 129.02, 126.54, 126.11, 125.37, 124.00, 123.73, 116.53, 106.22, 66.52, 40.84, 31.84, 27.42, 19.48. IR (NaCl): 3330.8, 2926.8, 2858.6, 1626.6, 1598.4, 1502.0, 1445.6, 1333.4, 1284.0, 1183.8, 1051.3, 968.1, 839.5, 804.2. HRMS (FAB+) calcd for $C_{18}H_{21}NO$ [M + H] 267.1623, found 267.1628. HPLC condition for determination of ee: Chiralcel OD, 0.8 mL min^{-1}, ^{n}hexane/^{i}PrOH = 95: 5, t_{R1} = 38.7 min, t_{R2} = 48.3 min, 96.0% ee. $[\alpha]^{22}_D$ = −23.8 (*c* 0.20, CH_2Cl_2).

(+)-CHANA: (+)-3-(6-Dimethylamino-2-naphthyl)-2-cyclohexenol. This enantiomer was obtained using the above procedure with exception of using (*R,R*)-*N*-*p*-tosyl-1,2-diphenylethylenediamine, affording the desired product as a yellow powder (12% yield, 98.0% ee) together with ketone (71% yield). ^{1}H NMR (400 MHz, $CDCl_3$): δ 7.73−7.65 (m, 2H), 7.60 (d, J = 8.4 Hz, 1H), 7.51 (dd, J_1 = 8.8 Hz, J_2 = 2.0 Hz, 1H), 7.15 (dd, J_1 = 9.2 Hz, J_2 = 2.4 Hz, 1H), 6.89 (d, J = 2.0 Hz, 1H), 6.24 (pseudo t, J = 2.0 Hz, 1H), 4.43 (m, 1H), 3.05 (s, 6H), 2.65−2.42 (m, 2H), 2.05−1.88 (m, 2H), 1.85−1.65 (m, 2H), 1.53−1.48 (m, 1H). ^{13}C NMR (75 MHz, $CDCl_3$): δ 148.71, 140.05, 134.59, 134.42, 129.03, 126.57, 126.13, 125.39, 124.02, 123.75, 116.54, 106.24, 66.53, 40.84, 31.86, 27.44, 19.49. IR (NaCl): 3416.9, 2930.1, 2851.2, 1625.1, 1597.5, 1502.3, 1450.0, 1323.0, 1286.6, 1184.2, 1038.4, 980.1, 830.6, 806.5. HRMS (FAB+) calcd for $C_{18}H_{21}NO$ [M + H] 267.1623, found 267.1636. HPLC condition for determination of ee: Chiralcel OD, 0.8 min^{-1}, ^{n}hexane/^{i}PrOH = 95: 5, t_{R1} = 38.7 min, t_{R2} = 48.3 min, 98.0% ee. $[\alpha]^{22}_D$ = +22.8 (*c* 0.20, CH_2Cl_2).

The reduction of CHANK to (±)-CHANA was achieved as described previously (*18*).

Enzyme Kinetics. To a black 96-well plate were added 0.1 M potassium phosphate buffer (pH 9) (188 μL), NAD^+ (8 μL of 12.5 mM stock, 500 μM final concentration), and 2 μL of CHANA in DMSO to achieve an assay concentration of 3K_m to K_m/3 and 2 μL of diluted HSD10 (0.08−1.5 μg), depending on the kinet-

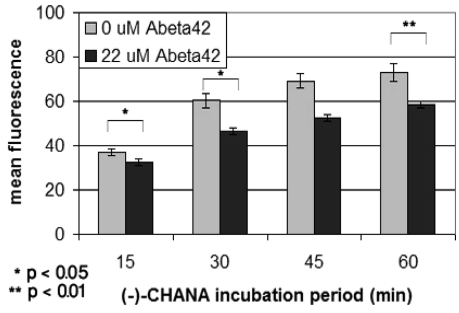

Figure 7. Inhibition of (−)-CHANA activity in amyloid-treated HEK293 cells. Cells were transfected with MTS-HSD10 for 24 h and then treated with 0 or 22 μM Aβ42 for 24 h before incubating with 2 μM (−)-CHANA and being imaged using confocal microscopy.

ics of the substrate. Fluorescence arising from the formation of product was monitored over the course of 30 min with excitation of 385 nm and emission of 510 nm.

Cell Culture. HEK 293T cells were grown in Dulbecco's modified Eagle medium (DMEM, Sigma) with 4 mM L-glutamine (Invitrogen) and 10% heat-inactivated fetal bovine serum (FBS) (Atlanta Biologicals).

HEK293T cells were grown in minimum essential medium (MEM, Sigma) supplemented with 10% (v/v) FBS, nonessential amino acids (Sigma), L-glutamine (2 mM), penicillin (100 units mL^{-1}), and streptomycin (0.1 mg mL^{-1})

SK-N-SH cells were grown in DMEM supplemented with 10% (v/v) FBS, L-glutamine (2 mM), penicillin (100 units mL^{-1}), and streptomycin (0.1 mg mL^{-1}). Alternatively, SK-N-SH cells were grown in DMEM with 4 mM L-glutamine and 10% (v/v) heat-inactivated FBS.

Mouse embryonic day 14 (E14) cortical neurons were cultured in MEM supplemented with 10% (v/v) FBS and 10% (v/v) horse serum. After 24 h the medium was replaced with MEM supplemented with serum-replacement-2 (Sigma) and 80 μM 5-fluorodeoxyuridine to inhibit proliferation of non-neuronal cells.

Western Blotting. Cells were washed in phosphate buffered saline (PBS, 2 × 3 min), harvested in lysis solution (50 μL for 35 mm dish, 100 μL for 60 mm dish) containing protease inhibitor cocktail (1×, Sigma), 8 M urea, 4.7% w/v CHAPS, 1% w/v DTT, and 1.5 μM PMSF and sonicated (60 Hz, 3 × 3 s). After sitting on ice (15 min), samples were centrifuged (13,000 × *g*, 5 min) to remove debris, and the supernatant was added to an equal volume of 2× protein sample buffer (2% (w/v) SDS, 20% (v/v) glycerol, 20 mM Tris, 20 mM EDTA, 0.239 M β-mercaptoethanol, 1 μg mL^{-1} bromophenol blue) and boiled for 10 min.

Samples were run on 10- or 15-well NuPAGE 4−12% Bis-Tris gels (Invitrogen) or 15 well Precise 8−16% Bis-Tris gels (Pierce, ThermoScientific) in MES buffer (45 min, 200 V). See-Blue Plus2 prestained standard (Invitrogen) was used as a molecular weight marker. Proteins were then transferred onto a nitrocellulose membrane (Whatman) at 30 V for 1 h using NuPAGE transfer buffer (Invitrogen). Protein transfer was confirmed by staining with Ponceau S solution (0.1% w/v Ponceau S, 5% acetic acid). Ponceau stain was removed by washing with tris-buffered saline (TBS).

Membranes were blocked in 5% w/v low-fat milk in Tris-buffered saline containing 0.1% Tween 20 (TBS-T, 1 h). The membrane was then incubated with anti-HSD10 (rabbit polyclonal, 1:6000 dilution, Sigma) in 3% milk in TBS containing 0.1% Tween20 (TBS-T, 4 °C, 16 h). The membrane was washed with TBT-T (3 × 5 min) before incubating with anti-rabbit HRP (goat, 1:20,000 dilution, Abcam) in 3% milk in TBS-T (5 mL, 30 min). The membrane was then washed with TBS-T (1 × 15 min, 2 × 5 min) and TBS (1 × 5 min) before incubating with SuperSignal West Pico enhanced chemiluminescence reagent (ECL; 4 mL, 5 min; Sigma) and detected using a chemiluminescence detector.

β-Actin was detected after stripping the membrane (10% acetic acid, 4 × 10 min) and blocking in 5% milk (1 h). The membrane was then incubated with anti-β-actin (mouse, 1:20,000 dilution, Sigma) in 3% milk in TBS-T (1 h). The membrane was washed with TBT-T (3 × 5 min) before incubating with anti-mouse HRP (goat, 1:20,000 dilution, Abcam) in TBS-T or 3% milk in TBS-T (5 mL, 30 min). The membrane was then washed with TBS-T (1 × 15 min, 2 × 5 min) and TBS (1 × 5 min) before incubating with SuperSignal West Pico enhanced chemiluminescence reagent (ECL; 4 mL, 5 min; Sigma) and detected using a chemiluminescence detector.

HSD10:actin ratios were calculated using Image J software (National Institutes of Health).

Fluorescence Imaging. For metabolism experiments, HEK293T cells were plated in a six-well dish at a density of 8.0×10^5 cells per well and were grown at 37 °C in 5% CO_2. After 24 h, cells were transfected, using Lipofectamine (Invitrogen) at a ratio of 5 μL of Lipofectamine to 1 μg DNA (pcDNA3, pcDNA3-HSD10). Approximately 24 h later, metabolism studies were initiated by changing media to DMEM minus phenol red (Invitrogen) supplemented with 4 mM L-glutamine, 1% charcoal/dextran-treated FBS (Atlanta Biologicals), and (+)-CHANA (15 μM) or (−)-CHANA (15 μM), all probes were prepared and stored as 5 mM stock solution in DMSO at 0 °C, stock solution was replaced weekly. Fluorescent images were taken at respective time points, 3 different images per well. Microscope filters were set at 585 nm: 493 ms; Brightfield: 37 ms. For each experiment, all images were adjusted using the same contrast ratios. Errors reported as standard error of the mean (SEM).

SK-N-SH cells were plated in a six-well dish at a density of 4.0×10^5 cells per well and were grown at 37 °C in 5% CO_2. After 24 h, cells were transfected with 1 μg of pcDNA3-HSD10, using Lipofectamine at a ratio of 5 μL of Lipofectamine to 1 μg DNA. The media was changed 6 h after transfection. Approximately 48 h later, the experiment was initiated by changing media to DMEM minus phenol red supplemented with 4 mM L-glutamine, 1% charcoal/dextran-treated FBS, and Probe (−)-CHANA (15 μM, prepared and stored as 5 mM stock solution in DMSO at 0 °C, stock solution was replaced weekly). Fluorescent images were taken at respective time points, with 3 different images per well. Microscope filters were set at 585 nm: 463 ms; and Brightfield: 37 ms. All images were adjusted using the same contrast ratios and mean fluorescent intensity (MFI) was calculated using Image J software.

Confocal Microscopy Studies. Cells were cultured on glass-bottomed 35 mm dishes (World Precision Instruments). Prior to imaging, medium was changed to phenol red-free medium [DMEM plus 4.5 g L^{-1} glucose, minus phenol red (Gibco), supplemented with 1% v/v charcoal-stripped fetal calf serum, penicillin (100 units mL^{-1}), streptomycin (0.1 mg mL^{-1}) and glutamine (2 mM)] and incubated with 2 μM (−)-CHANA (from 1 mM stock in DMSO) with images taken at set time points over 1 h. Fluorescence imaging was carried out using a heated stage (37 °C) on a Leica DM IRE2 inverted microscope with 405 nm diode laser and 40× oil objective at 200 Hz, averaged over 8 images. Samples were excited at 405 nm, and the emission was collected at 500−520 nm (HEK293) or 470−540 nm (SK-N-SH). Three images per dish were recorded, and three dishes were measured in separate experiments. Mean fluorescence intensities were calculated using ImageJ, with errors reported as SEM. Statistical analysis was performed using the Student's *t* test.

MitoTracker Staining. Cells were cultured in 35 mm glass-bottomed tissue culture dishes. Mitochondrial staining was performed using MitoTracker Deep Red (25−100 nM in DMEM, from 1 mM stock in DMSO, Invitrogen) at 37 °C for 20−40 min. Medium was changed to 2 μM (−)-CHANA for 1 h before imaging using a 63 × oil objective. MitoTracker staining was observed by excitation at 633 nm and emission 640−700 nm, (−)-CHANA excitation 405 nm and emission 470−540 nm.

HSD10 Overexpression for Confocal Microscopy Studies. Mitochondrial-targeted human HSD10 (MTS-HSD10) was cloned (forward primer GCCAAGCTTAGCATGTCCGTCCTGACGCCG; reverse primer CCGCTCGAGTCAAGGCTGCATACGAATGGC) and ligated into pcDNA3 using *Hind* III and *Xho* I restriction sites. The mitochondrial targeting sequence originated from pDsRed2-mito (Clontech). The resulting plasmid was transformed into *E. coli* DH5α cells and plasmid DNA extracted using a DNA mini-prep kit according to the manufacturer's instructions (Qiagen).

HEK293 cells were grown in 35 mm glass-bottomed dishes for 24 h before transfection with a plasmid encoding mitochondrial-targeted HSD10 (MTS-HSD10) (1 μg) using GeneJammer reagent (Stratagene). GeneJammer (3 μL) and Optimem medium (100 μL) were mixed and incubated for 5 min before addition of DNA (1 μg) and incubation for a further 20 min. The transfection mixture was added to the culture dishes and incubated for 24−48 h at 37 °C, 5% CO_2.

AG18051 Inhibition. SK-N-SH cells were prepared as indicated. Approximately 48 h after transfection, the media was removed and 1 mL of DMEM minus phenol red supplemented with 4 mM L-glutamine, 1% charcoal/dextran-treated FBS, containing AG18051 (2−5 μL of 10 μM−1 mM stock solution to achieve inhibitor concentration of 0.0−5.0 μM in the media, all stocks were prepared in DMSO) was added to each well. After 1 h, an additional 1 mL of media containing (−)-CHANA (30 μM; final probe concentration 15 μM) and AG18051 (2−5 μL of 10 μM−1 mM stock solution to achieve inhibitor concentration of 0.0−5.0 μM in the media) was added to each well. Images were taken after 6 h, using microscope filters as indicated for regular fluorescent experiments. All experiments were run in duplicate with three images taken per well.

Amyloid Inhibition Studies. Aβ42 (Innovagen) was monomerised by treatment with 1,1,1,3,3,3-hexafluoroisopropanol (HFIP) (*22*) (1 mg Aβ42 was dissolved in 1 mL of HFIP and incubated for 1 h at room temp before evaporating HFIP overnight). Aβ42 (0.1 mg) was dissolved in DMSO (10 μL) and sonicated in an ultrasonic bath (10 min) before dilution with culture medium to the appropriate concentration. Cells were treated with 0 or 22 μM Aβ42 for 24 h before imaging with (−)-CHANA as described above. At this concentration of Aβ42 there was no cell loss. Statistical analysis was performed using the Student's *t* test.

Supporting Information Available: This material is available free of charge *via* the Internet at http://pubs.acs.org.

Acknowledgment: This work was supported by the Alzheimer's Research Trust (a William Lindsay scholarship to K.E.A.M), National Science Foundation (a NSF predoctoral fellowship to M.F.) and the G. Harold & Leila Y. Mathers Charitable Foundation. S.J.C. thanks St Hugh's College, University of Oxford, Oxford, U.K. for research support.

REFERENCES

1. Yan, S. D., Fu, J., Soto, C., Chen, X., Zhu, H., Al-Mohanna, F., Collison, K., Zhu, A., Stern, E., Saido, T., Tohyama, M., Ogawa, S., Roher, A., and Stern, D. (1997) An intracellular protein that binds amyloid-β peptide and mediates neurotoxicity in Alzheimer's disease, *Nature 389*, 689–695.
2. Powell, A. J., Read, J. A., Banfield, M. J., Gunn-Moore, F., Yan, S. D., Lustbader, J., Stern, A. R., Stern, D. M., and Brady, R. L. (2000) Recognition of structurally diverse substrates by type II 3 hydroxyacyl-CoA dehydrogenase (HADH II)/amyloid-β binding alcohol dehydrogenase (ABAD), *J. Mol. Biol. 303*, 311–327.
3. Lustbader, J. W., Cirilli, M., Lin, C., Xu, H. W., Takuma, K., Wang, N., Caspersen, C., Chen, X., Pollak, S., Chaney, M., Trinchese, F., Liu, S., Gunn-Moore, F., Lue, L.-F., Walker, D. G., Kuppusamy, P., Zewier, Z. L., Arancio, O., Stern, D., Yan, S. S., and Wu, H. (2004) ABAD directly links A 102 to mitochondrial toxicity in Alzheimer's disease, *Science 304*, 448–452.
4. Kissinger, C. R., Rejto, P. A., Pelletier, L. A., Thomson, J. A., Showalter, R. E., Abreo, M. A., Agree, C. S., Margosiak, S., Meng, J. J., Aust, R. M., Vanderpool, D., Li, B., Tempczyk-Russell, A., and Villafranca, J. E. (2004) Crystal structure of human ABAD/HSD10 with a bound inhibitor: implications for design of Alzheimer's disease therapeutics, *J. Mol. Biol. 342*, 943–952.
5. He, X.-Y., Merz, G., Mehta, P., Schulz, H., and Yang, S.-Y. (1999) Human brain short chain L-3-hydroxyacyl coenzyme A dehydrogenase is a single-domain multifunctional enzyme. Characterization of a novel 17-β-hydroxysteroid dehydrogenase, *J. Biol. Chem. 274*, 15014–15019.
6. Oppermann, U. C. T., Salim, S., Tjernberg, L. O., Terenius, L., and Jornvall, H. (1999) Binding of amyloid β-peptide to mitochondrial hydroxyacyl-CoA dehydrogenase (ERAB): regulation of an SDR enzyme activity with implications for apoptosis in Alzheimer's disease, *FEBS Lett. 451*, 238–242.
7. Yan, S. D., Shi, Y., Zhu, A., Fu, J., Zhu, H., Zhu, Y., Gibson, L., Stern, E., Collison, K., Al-Mohanna, F., Ogawa, S., Roher, A., Clarke, S. G., and Stern, D. M. (1999) Role of ERAB/L-3-hydroxyacyl-coenzyme A dehydrogenase type II activity in Aβ-induced cytotoxicity, *J. Biol. Chem. 274*, 2145–2156.
8. He, X. Y., Yang, Y. Z., Schulz, H., and Yang, S. Y. (2000) Intrinsic alcohol dehydrogenase and hydroxysteroid dehydrogenase activities of human mitochondrial short-chain L-3-hydroxyacyl-CoA dehydrogenase, *Biochem. J. 345*, 139–143.
9. Yang, S.-Y., He, X.-Y., and Schulz, H. (2005) 3-Hydroxyacyl-CoA dehydrogenase and short chain-3-hydroxyacyl-CoA dehydrogenase in human health and disease, *FEBS J. 272*, 4874–4883.
10. Muirhead, K. E., Borger, E., Aitken, L., Conway, S. J., and Gunn-Moore, F. J. (2010) The consequences of mitochondrial amyloid β-peptide in Alzheimer's disease, *Biochem. J. 426*, 255–70.
11. He, X.-Y., Schulz, H., and Yang, S.-Y. (1998) A human brain L-3-hydroxyacyl-coenzyme A dehydrogenase is identical to an amyloid β-peptide-binding protein involved in Alzheimer's disease, *J. Biol. Chem. 273*, 10741–10746.
12. Ofman, R., Jos Ruiter, P. N., Feenstra, M., Duran, M., Bwee Poll-The, T., Zschocke, J., Ensenauer, R., Lehnert, W., Sass, J. O., Sperl, W., and Ronald Wanders, J. A. (2003) 2-Methyl-3-hydroxybutyryl-CoA dehydrogenase deficiency is caused by mutations in the HADH2 gene, *Am. J. Hum. Genet. 72*, 1300–1307.
13. He, X.-Y., Wegiel, J., Yang, Y.-Z., Pullarkat, R., Schulz, H., and Yang, S.-Y. (2005) Type 10 17β-hydroxysteroid dehydrogenase catalyzing the oxidation of steroid modulators of γ-aminobutyric acid type A receptors, *Mol. Cell. Endocrinol. 229*, 111–117.
14. Takuma, K., Yao, J., Huang, J., Xu, H., Chen, X., Luddy, J., Trillat, A.-C., Stern, D. M., Arancio, O., and Yan, S. S. (2005) ABAD enhances Aβ-induced cell stress via mitochondrial dysfunction, *FASEB J. 19*, 597–598.
15. Yan, Y., Liu, Y., Sorci, M., Belfort, G., Lustbader, J. W., Yan, S. S., and Wang, C. (2007) Surface plasmon resonance and nuclear magnetic resonance studies of ABAD-Aβ interaction, *Biochemistry 46*, 1724–1731.
16. Yao, J., Taylor, M., Davey, F., Ren, Y., Aiton, J., Coote, P., Fang, F., Chen, J. X., Yan, S. D., and Gunn-Moore, F. J. (2007) Interaction of amyloid binding alcohol dehydrogenase/Aβ mediates up-regulation of peroxiredoxin II in the brains of Alzheimer's disease patients and a transgenic Alzheimer's disease mouse model, *Mol. Cell. Neurosci. 35*, 377–382.
17. Ren, Y., Xu, H. W., Davey, F., Taylor, M., Aiton, J., Coote, P., Fang, F., Yao, J., Chen, D., Chen, J. X., Yan, S. D., and Gunn-Moore, F. J. (2008) Endophilin I expression is increased in the brains of Alzheimer disease patients, *J. Biol. Chem. 283*, 5685–91.
18. Froemming, M. K., and Sames, D. (2007) Harnessing functional plasticity of enzymes: a fluorogenic probe for imaging 17β-HSD10 dehydrogenase, an enzyme involved in Alzheimer's and Parkinson's diseases, *J. Am. Chem. Soc. 129*, 14518–22.
19. Hashiguchi, S., Fujii, A., Haack, K.-J., Matsumura, K., Ikariya, T., and Noyori, R. (1997) Kinetic resolution of racemic secondary alcohols by Ru^{II}-catalyzed hydrogen transfer, *Angew. Chem., Int. Ed. Engl. 36*, 288–290.
20. Luche, J.-L., Rodriguez-Hahn, L., and Crabbe, P. (1978) Reduction of natural enones in the presence of cerium trichloride, *J. Chem. Soc., Chem. Commun.* 601–602.

21. Frackowiak, J., Mazur-Kolecka, B., Kaczmarski, W., and Dickson, D. (2001) Deposition of Alzheimer's vascular amyloid-β is associated with decreased expression of brain L-3-hydroxyacyl-coenzyme A dehydrogenase (ERAB), *Brain Res. 907*, 44–53.
22. Klein, W. L. (2002) Aβ toxicity in Alzheimer's disease: globular oligomers (ADDLs) as new vaccine and drug targets, *Neurochem. Int. 41*, 345–352.